Observations, Roche Lobe Analysis, and Period Study of the Eclipsing Contact Binary System GM Canum Venaticorum

Kevin B. Alton
UnderOak Observatory, 70 Summit Avenue, Cedar Knolls, NJ; kbalton@optonline.net

Robert H. Nelson
Mountain Ash Observatory, 1349 Garvin Street, Prince George, BC V2M 3Z1, Canada
Guest Investigator, Dominion Astrophysical Observatory Herzberg Institute of AstrophysicsNational Research Council of Canada

Received January 24, 2018; revised March 23, 2018; accepted March 28, 2018

Abstract GM CVn is an eclipsing W UMa binary system (P = 0.366984 d) which has been largely neglected since its variability was first detected during the ROTSE-I campaign (1999–2000). Other than a single unfiltered light curve (LC) no other photometric data have been published. LC data collected in three bandpasses (B, V, and R_c) at UnderOak Observatory (UO) produced three new times of minimum for GM CVn. These along with other eclipse timings from the literature were used to update the linear ephemeris. Roche modeling to produce synthetic LC fits to the observed data was accomplished using BINARY MAKER 3, WDWINT56A, and PHOEBE v.31a. Newly acquired radial velocity data were pivotal to defining the absolute and geometric parameters for this partially eclipsing binary system. An unspotted solution achieved the best Roche model fits for the multi-color LCs collected in 2013.

1. Introduction

The variable behavior of GM CVn (GSC 2545-0970) was first observed during the ROTSE-I CCD survey (Akerlof *et al.* 2000); these photometric determinations are available on the Northern Sky Variable Survey website (Wozniak *et al.* 2004). The same data were analyzed later in more detail by Gettel *et al.* (2006), while an ephemeris was reported by Blättler and Diethelm (2006) based on new unfiltered light curve (LC) results. Although times of minimum light have been sporadically published since 2005, this paper marks the first detailed period analysis, spectroscopic study, and multi-color Roche model assessment of LCs for this system in the literature.

2. Observations and data reduction

2.1. Photometry

Photometric collection dates (UTC) at UnderOak Observatory (UO) included seven sessions between 05 May 2013 and 31 May 2013, with an additional imaging run captured on 05 June 2013. Equipment included a 0.2-m Schmidt-Cassegrain telescope with an SBIG ST-8XME CCD camera mounted at the Cassegrain focus. Automated imaging was performed with photometric B, V, and R_c filters sourced from SBIG and manufactured to match the Bessell prescription; the exposure time for all dark- and light-frames was 60 seconds. The computer clock was updated automatically via the U.S. Naval Observatory Time Server immediately prior to each session. Image acquisition (lights, darks, and flats) was performed using CCDSOFT v5 (Software Bisque 2011) while calibration and registration were performed with AIP4WIN v2.4.0 (Berry and Burnell 2005). Images of GM CVn were plate-solved using the standard star fields (MPOSC3) provided in MPOCANOPUS v10.7.1.3 (Minor Planet Observer 2015) in order to obtain the magnitude (B, V, and R_c) assignments for each comparison star. Reduction to magnitudes was accomplished using aperture photometry on a fixed ensemble of five non-varying comparison stars in the same field-of-view (FOV). Only images taken above 30° altitude (airmass < 2.0) were accepted in order to minimize the effects of differential refraction and color extinction.

2.2. Light curve analyses

Roche-type modeling was initially performed using BINARY MAKER 3.03 (BM3; Bradstreet and Steelman 2002). Thereafter, WDWINT56A (Nelson 2009) and PHOEBE v.31a (Prša and Zwitter 2005), both of which employ the Wilson-Devinney (WD) code (Wilson and Devinney 1971; Wilson 1990), were used to refine the fit and estimate parameter errors. A rendering of the Roche surface from GM CVn was produced by BM3 once model fitting was finalized. Times of minimum were calculated using the method of Kwee and van Woerden (1956) as featured in PERANSO v2.5 (Paunzen and Vanmunster 2016).

2.3. Spectroscopic observations

A total of ten medium-resolution (mean R ~ 10,000) spectra of GM CVn were acquired at the Dominion Astrophysical Observatory (DAO) in Victoria, British Columbia, Canada, between 09 April and 18 April 2017. For this study a Cassegrain spectrograph with a grating (#21181; 1,800 lines/mm) blazed at 5000 Å was installed on the 1.85-m "Plaskett" telescope. This provided a reciprocal first order linear dispersion of 10 Å/mm that approximately covered a wavelength region between 5000 and 5260 Å. Other specifics regarding the instrument and data processing are detailed elsewhere (Nelson 2010a).

3. Results and discussion

3.1. Photometry and ephemerides

A summary of the five stars in the same FOV with GM CVn used to derive catalog-based (MPOSC3) magnitudes in MPOCANOPUS is provided in Table 1. During each image acquisition session comparison stars typically stayed within ±0.014 mag for V and R_c filters and ±0.03 mag for B passband.

Table 1. Astrometric coordinates (J2000) and color indices (B–V) for GM CVn and five comparison stars used in this photometric study.

Star Identification	*R. A.* h m s	*Dec.* ° ' "	*MPOSC3*[a] *(B–V)*
GM CVn	14 02 46.63	32 08 47.9	0.618
TYC 2545-0240-1	14 02 05.69	32 08 01.8	0.521
TYC 2545-1027-1	14 02 05.69	32 11 49.1	0.598
TYC 2545-0285-1	14 01 22.44	32 17 24.9	1.131
TYC 2545-0235-1	14 01 04.29	32 16 04.8	0.502
GSC 02545-0759	14 01 58.48	32 06 24.1	0.660

a. MPOSC3 is a hybrid catalog which includes a large subset of the Carlsberg Meridian Catalog *(CMC-14) as well as data from the* Sloan Digital Sky Survey *(SDSS). Stars with BVR$_c$ magnitudes derived from 2MASS J–K magnitudes have an internal consistency of ± 0.05 mag. for V, ± 0.08 mag. for B, ± 0.03 mag. for Rc , and ± 0.05 mag. for B–V (Warner 2007).*

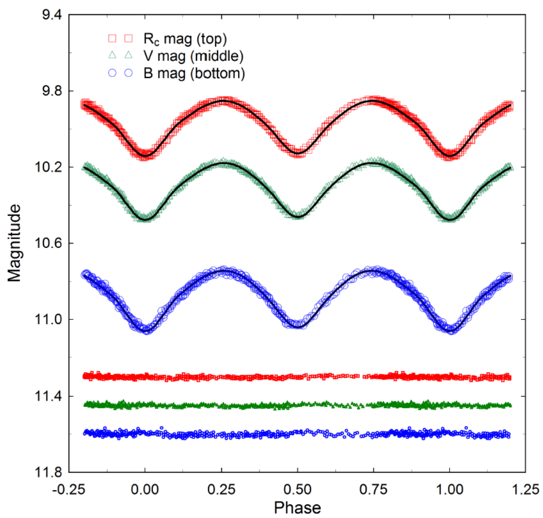

Figure 1. Folded CCD light curves for GM CVn produced from photometric data obtained between 05 May and 05 June 2013. The top (R$_c$), middle (V), and bottom (B) curves shown above were reduced to MPOSC3-based catalog magnitudes using MPOCANOPUS. The light curves are shallow and lack a total eclipse so the WD solution required simultaneous modeling with radial velocity data. In this case, the Roche model assumed a W-subtype contact binary with no spots; residuals from the model fits are offset at the bottom of the plot to keep the values on scale.

Photometric values in B (n = 332), V (n = 341), and R$_c$ (n = 345) passbands were separately processed to produce LCs that spanned 31 days in between 05 May and 05 June 2013 (Figure 1). These determinations included three new times of minimum for each filter and since there was no obvious color dependency on the timings, all data were averaged (Table 2) from each session. The Fourier routine (FALC; Harris *et al.* 1989) in MPOCANOPUS produced a slightly longer period solution (0.366996 ± 0.000001 d) after initially seeding the analysis with the orbital period (0.366986 d) from the ephemeris (Equation 1) derived by Blättler and Diethelm (2006). An independent verification of all period determinations was performed using PERANSO v2.5 (Paunzen and Vanmunster 2016) by applying periodic orthogonals (Schwarzenberg-Czerny 1996) to fit observations and analysis of variance (ANOVA) to assess fit quality. In this case a similar period solution (0.366995 ± 0.000012 d) was obtained. Finally, folding together (time span = 5,173 d) the sparsely sampled ROTSE-I data with those (V-mag) acquired at UO yielded a period at 0.366984 ± 0.000012 d. New minima acquired at UO along with published values starting in 2005 (Table 2) were used to analyze eclipse timings through 2016 when the latest time of minimum was reported in the literature. The reference epoch (Blättler and Diethelm 2006) employed for calculating ET differences (ETD) was defined by the following linear ephemeris Equation 1:

Table 2. Calculated differences (ETD)$_I$ following linear least squares fit of observed times-of-minimum for GM CVn and cycle number between 12 Jan 2005 and 17 Mar 2016.

HJD = 2400000+	*Cycle No.*	*ETD$_I$*[a]	*Reference*
53382.5390	–327	–0.004378	Diethelm 2006
53382.7261	–326.5	–0.000771	Diethelm 2006
53445.4833	–155.5	0.001823	Diethelm 2006
53463.4644	–106.5	0.000609	Diethelm 2006
53502.3652	–0.5	0.000893	Diethelm 2006
53502.5476	0	–0.000200	Diethelm 2006
53502.5478	0	0.000000	Blättler and Diethelm 2006
53515.3925	35	0.000190	Diethelm 2006
53515.5758	35.5	–0.000003	Diethelm 2006
53517.4118	40.5	0.001067	Diethelm 2006
53936.5091	1182.5	0.000355	Diethelm 2007
54174.4923	1831	–0.006866	Diethelm 2007
54856.9018	3690.5	–0.007833	Nelson 2010b
54857.0824	3691	–0.010726	Nelson 2010b
54936.7183	3908	–0.010788	Nelson 2010b
55015.4361	4122.5	–0.011485	Diethelm 2010
55560.9579	5609	–0.014374	Nelson 2011
56014.7339	6845.5	–0.016563	Nelson 2013a
56069.4179	6994.5	–0.013477	Hübscher and Lehmann 2013
56408.5114	7918.5	–0.015041	Hübscher 2013
56418.4159	7945.5	–0.019163	Hübscher 2013
56418.5992	7946	–0.019314	This study
56439.6980	8003.5	–0.022247	This study
56448.6917	8028	–0.019749	This study
57021.0020	9587.5	–0.024075	Nelson 2015
57115.4993	9845	–0.025670	Bahar *et al.* 2017
57119.5361	9856	–0.025716	Hübscher 2017
57352.0223	10489.5	–0.025147	Nelson 2016
57464.5003	10796	–0.028356	Hübscher 2017

a. (ETD)$_I$ = Eclipse Time Difference between observed time-of-minimum and that calculated using the reference ephemeris (Blättler and Diethelm 2006).

$$Min.\ I\ (HJD) = 2453502.5478 + 0.366986\ E. \qquad (1)$$

Variations in orbital period over time can potentially be uncovered by plotting the difference between the observed eclipse times and those predicted by the reference epoch against cycle number (Figure 2). Thus far, all of the calculated ETD values basically describe a straight line relationship and suggest that little or no change to the period has occurred since 2005. The improved ephemeris (Equation 2) based on eclipse timing data available through March 2016 is as follows:

$$Min.\ I\ (HJD) = 2457464.5020(5) + 0.3669835(1)\ E. \qquad (2)$$

Given that these data cover a relatively short span of time (~12 yr) there is always the possibility that significant orbital period changes in the system had not occurred within this interval. Future times of minimum could potentially reveal residuals consistent with the gravitational influence of a third (or more) body, star-spot cycles (Applegate 1992), or periodic mass transfer between either star.

3.2. Light curve behavior

The phasing of the light curves reveals that GM CVn is tidally locked as expected for a W UMa eclipsing binary (Figure 1). The primary and secondary maxima are equal; this classically indicates that there are no major spots at the present (Yakut and Eggleton 2005). In contrast to the 2013 LCs, unfiltered photometric data taken during the ROTSE-I CCD survey and later by Blätter and Dielthelm (2006) did exhibit unequal heights (Max I > Max II), which indicates that this system like most other contact binaries is photospherically active (Figure 3).

3.3. Spectral classification

The interstellar extinction (A_V) was estimated for GM CVn according to the approach described by Amôres and Lépine (2005). This model, which is simulated in a companion program (ALEXTIN: http://www.galextin.org/explain.html) for targets within the Milky Way Galaxy, requires the galactic coordinates (*l, b*) and an estimated distance in kpc. In this case the value for A_V (0.024) corresponds to a target positioned at l = 55.348° and b = +73.936° which is located within 200 pc (see section 3.8). The dust maps rendered by Schlegel *et al.* (1998) and later refined by Schlafly and Finkbeiner (2011) determine extinction based on total dust in a given direction and not extinction within a certain distance. Therefore, reddening values for objects like GM CVn closer than 1 kpc tend to be overestimated (A_V = 0.045; E(B–V) = 0.0145) particularly as they approach the galactic plane. Color index (B–V) data collected at UO and those acquired from an ensemble of eight other sources (Table 3) were corrected using the reddening value estimated by factoring in distance. The median result ($(B–V)_0$ = 0.588 ± 0.027) which was adopted for Roche modeling indicates a primary star with an effective temperature (5920 K) that ranges in spectral type between F9V and G0V.

3.4. Spectroscopic observations

A log of all spectra captured between 09 April and 18 April 2017 is provided in Table 4, while two representative sample spectra are illustrated in Figure 4. Spectral reduction was performed using the application RAVERE (Nelson 2010c). This software includes the ability to manually remove trace cosmic hits, produce a median background fit for each column (or wavelength), perform aperture summation and background subtraction for each column, and normalize the continuum. Final extraction of the RV data employed broadening functions (BROAD; Nelson 2013b) to improve peak resolution. Further details regarding the advantage of using wavelength broadening functions for contact binary systems rather than cross-correlation

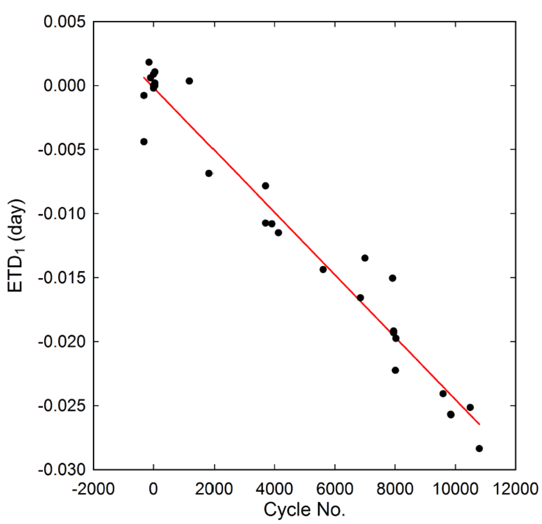

Figure 2. Straight line fit (ETD vs. period cycle number) suggesting that little or no change to the orbital period of GM CVn had occurred between 2005 and 2016.

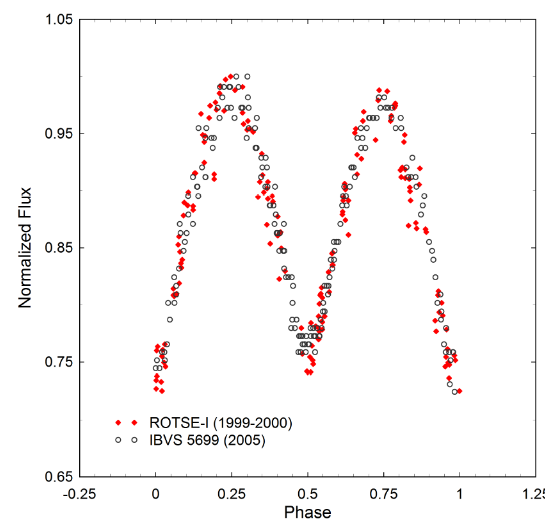

Figure 3. Folded (unfiltered) light curves (P = 0.366986 ± 0.000045 d) for GM CVn illustrating peak asymmetry (Max I > Max II) observed during quadrature in 1999–2000 (ROTSE-I; Akerlof *et al.* 2000) and in 2005 (Blättler and Diethelm 2006).

Table 3. Spectral classification of GM CVn based upon dereddened (B–V) data from eight surveys and the present study.

	USNO-B1.0	*All Sky Combined*	*2MASS*	*USNO A2*	*SDSS-DR9*	*Tycho*	*UCAC4*	*HIP/Tycho*	*Present Study*
$(B–V)_0$	0.515	0.611	0.610	0.500	0.621	0.588	0.542	0.609	0.561
T_{eff1} [a] (K)	6218	5863	5865	6278	5839	5921	6089	5867	6009
Spectral Class[a]	F7-F8V	G1-G2V	G1-G2V	F6-F7V	G1-G2V	F9-G0V	F8-F9V	G1-G2V	F9-G0V

a. T_{eff1} interpolated and spectral class assigned from Pecaut and Mamajek (2013). Median value, $(B–V)_0$ = 0.588 ± 0.027, corresponds to an F9V-G0V primary star (T_{eff1} = 5920 K).

Table 4. A log of spectral observations at the DAO in April 2017.

DAO Image #	*Mid-time (HJD = 2400000+)*	*Exposure (s)*	*Phase at Mid-exp.*	*V_2 (km/s)*	*V_1 (km/s)*
3921	57852.8978	1748	0.370	-208.6 ± 2.0	37.70 ± 1.8
3938	57854.7431	157	0.398	-172.5 ± 3.6	25.95 ± 5.3
3958	57854.8960	1800	0.815	196.2 ± 3.7	-97.5 ± 3.7
3998	57859.8229	1800	0.240	-254.7 ± 1.7	56.0 ± 0.6
4032	57861.8914	600	0.876	149.0 ± 3.2	-87.8 ± 2.5

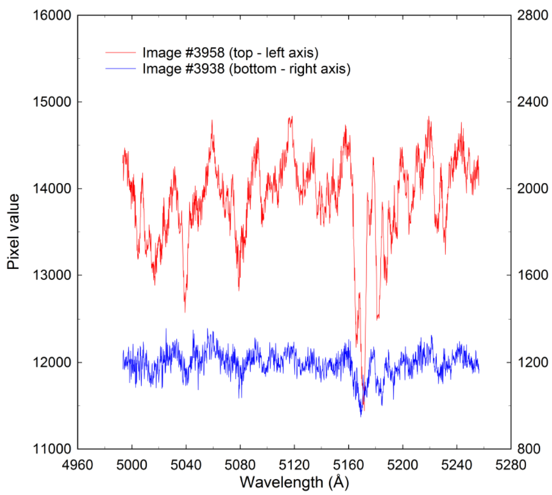

Figure 4. Representative spectra collected at DAO to determine radial velocities for GM CVn at φ = 0.398 (Image # 3938) and φ = 0.815 (Image # 3958).

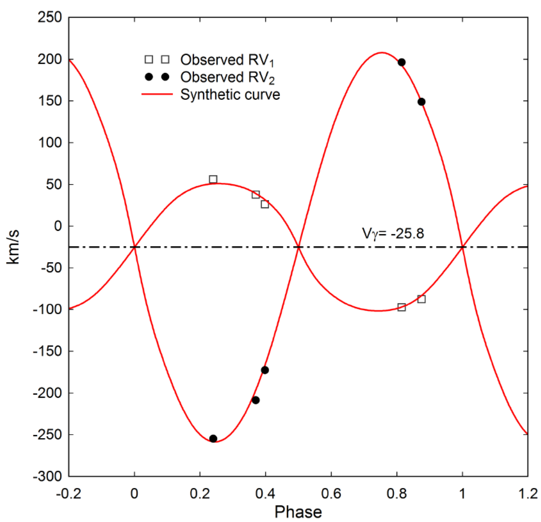

Figure 5. Best fit radial velocity curve produced following simultaneous WD modeling (WDWINT56A) with LC data. RMS error (2.72 km/s) for the synthetic RV curve indicated a good fit to the observed velocity data.

is described elsewhere (Ruciński 2004). Arguably, more data might dispel concerns about the robustness of the RV model fits; however, we feel confident about the final results from these ten values given the high precision of the velocity determinations and the relatively low rms (2.72 km/s) calculated for the model fits.

3.5. Roche modeling approach

The newly acquired radial velocity (RV) data reported herein (Table 4; Figures 4 and 5) for the first time were necessary to obtain a unique solution for the mass ratio (m_2/m_1), determine a value for the total mass, and unequivocally determine whether GM CVn is an A-type or W-type contact binary system. Aside from initial modeling with BM3 (Bradstreet and Steelman 2002), Roche modeling of LC data from GM CVn was primarily accomplished using the programs PHOEBE v.31a (Prša and Zwitter 2005) and WDWINT56A (Nelson 2009), both of which feature a user-friendly interface to the Wilson-Devinney (WD) code (Wilson and Devinney 1971; Wilson 1990). WDWINT56A makes use of Kurucz's atmosphere models (Kurucz 2000) which are integrated over UBVR$_c$I$_c$ optical passbands. In both cases, the selected model was Mode 3 for an over-contact binary. Bolometric albedo ($A_{1,2} = 0.5$) and gravity darkening coefficients ($g_{1,2} = 0.32$) for cooler stars (7500 K) with convective envelopes were respectively assigned according to Ruciński (1969) and Lucy (1967). Logarithmic limb darkening coefficients (x_1, x_2, y_1, y_2) were interpolated (van Hamme 1993) following any change in the effective temperature (T_{eff2}) of the secondary star during model fit optimization. According to the putative classification of GM CVn as spectral type F9V to G0V the effective temperature of the more massive star was fixed ($T_{eff1} = 5920$ K). Direct least-squares sinusoidal curve fitting of the RV data was initially carried out with an EXCEL spreadsheet designed by RHN using a custom macro and the Solver add-in. These preliminary results led to values for the radial velocities ($v_{1r} = 241.05$ km/s and $v_{2r} = 82.93$ km/s), q = 0.344, and the systemic velocity ($V_\gamma = -24.41$ km/s). Subsequently, RV and LC data (V-mag only) were simultaneously modeled using WDWINT56A in order to obtain initial estimates for K_1, K_2, q, the semi-major axis (SMA), and V_γ. All but the temperature of the more massive star (T_{eff1}), orbital period (P = 0.366984 d), $A_{1,2}$, and $g_{1,2}$ were allowed to vary during DC iterations. In general, the best fits for T_{eff2}, i, and Roche potentials ($\Omega_1 = \Omega_2$) were collectively refined (method of multiple subsets) by DC before attempts were made to simultaneously optimize $\Omega_{1,2}$, i, T_{eff2}, q, V_γ, and the SMA. Once the Roche model fit was optimized using the monochromatic LC data, the other LCs (B and R_c) were added to the model. Hereafter T_{eff1} remained fixed while simultaneously varying T_{eff2}, i, q, V_γ, SMA, and the Roche potential ($\Omega_1 = \Omega_2$) to obtain a best fit for the multicolor data. Synthesis of light curves for GM CVn with good fits during quadrature (Max I ~ Max II) and around minimum light (Min I and Min II) were possible without the incorporation of a spot.

3.6. Roche modeling results

According to the convention employed herein, the primary star (m_1) is considered the more massive, thus, the best fit for the mass ratio (m_2/m_1) was observed at q = 0.341 ± 0.001. In order to accommodate this definition, the LC phase had to be shifted (φ ± 0.5) to properly align the RV and LC data. Simultaneous Roche modeling of RV and LC data demonstrates that GM CVn is a W-type contact binary system (Figure 1) in which the smaller but slightly hotter star is eclipsed (in this case partially) by its cooler but larger orbital partner. These results are consistent with the general observation (Csizmadia and Klagyivik 2004; Skelton and Smits 2009) that W-type eclipsing binaries have a mass ratio $m_2/m_1 > 0.3$, are equal to or cooler than the Sun with spectral types ranging from G to K, and orbit each other with periods varying between 0.22 to 0.4 day. A pictorial model rendered with BM3 using the physical and geometric elements from the best fit Roche model is shown in Figure 6. The LC parameters and geometric elements determined for each of these model fits are summarized in Table 5. It should be noted that the listed errors only reflect the model fit to the observations which assumed exact values for all fixed parameters.

The fill-out parameter (f), which corresponds to a volume percent of the outer surface shared between each star, was calculated according to Equation 3 (Kallrath and Malone 1999; Bradstreet 2005) where:

$$f = (\Omega_{inner} - \Omega_{1,2} / (\Omega_{inner} - \Omega_{outer}), \qquad (3)$$

Ω_{outer} is the outer critical Roche equipotential, Ω_{inner} is the value for the inner critical Roche equipotential, and $\Omega = \Omega_{1,2}$ denotes the common envelope surface potential for the binary system. In this case the constituent stars are in shallow contact ($f < 15\%$) as defined by He and Qian (2009). The evolutionary track for GM CVn is probably similar to that described for V608 Cas (Liu *et al.* 2016), another W-type shallow-contact binary system with a mass ratio ($q = 0.343$) similar to GM CVn. Shallow-contact W UMa variables are believed to be in an evolutionary path between deep contact and near contact binary stars. When a semi-detached binary evolves inward as a result of mass transfer and/or angular momentum loss (Bradstreet and Guinan 1994) it can evolve into a contact system. Others have argued (Liu *et al.* 2010) that deep-contact binaries may evolve to shallow-contact systems by thermal relaxation oscillation (TRO) and could ultimately reach a broken-contact phase. Additional photometric studies on GM CVn could prove invaluable to understanding the evolutionary status of this system.

3.7. Absolute parameters

Absolute parameters (Table 6) were derived for each star in this W-type W UMa binary system using results from the unspotted model simulation. Apart from a spectroscopic mass ratio (q_{sp}), the other critical values provided by RV data are the orbital speeds ($v_{1r} + v_{2r}$). As such, the total mass can be calculated according to Equation 4 when the orbital inclination (i) is known:

$$(m_1 + m_2) \sin^3 i = (P / 2\pi G)(v_{1r} + v_{2r})^3. \qquad (4)$$

From the simultaneous fit of LC and RV data, $V_\gamma = -25.8 \pm 0.29$ km/s, $v_{2r} = 236.9 \pm 5.45$ km/s, $v_{1r} = 76.55 \pm 6.16$ km/s, and $i° = 63.07 \pm 0.06$. The total mass of the system was determined to be $1.65 \pm 0.09\ M_\odot$ and since $q = 0.341$, the primary mass $= 1.23 \pm 0.06\ M_\odot$ and the secondary mass $= 0.42 \pm 0.02\ M_\odot$. A stand-alone star with a mass similar to the secondary would likely be classified as an early M-type. The semi-major axis, $a(R_\odot) = 2.55 \pm 0.04$, was calculated from Newton's version (Equation 5) of Kepler's third law where:

$$a^3 = (G \times P^2 (M_1 + M_2)) / (4\pi^2). \qquad (5)$$

The effective radii of each Roche lobe (r_L) can be calculated to over the entire range of mass ratios ($0 < q < \infty$) according to the expression (6) derived by Eggleton (1983):

$$r_L = (0.49q^{2/3}) / (0.6q^{2/3} + \ln(1 + q^{1/3})), \qquad (6)$$

from which values for r_1 (0.4739 ± 0.0003) and r_2 (0.2908 ± 0.0002) were determined for the primary and secondary stars, respectively. Since the semi-major axis and the volume radii are known, the solar radii for both binary constituents can be calculated where $R_1 = a \cdot r_1 = (1.21 \pm 0.02\ R_\odot)$ and $R_2 = a \cdot r_2 = (0.74 \pm 0.01\ R_\odot)$.

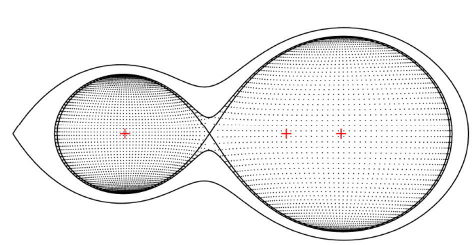

Figure 6. Surface model (φ = 0.25) of GM CVn showing the Roche lobe outlines for this shallow contact W-type W UMa eclipsing binary system.

Table 5. Synthetic light curve parameters employed for Roche modeling and the geometric elements determined for GM CVn, a W-type W UMa variable.

Parameter	*Value*
T_{eff1} (K)[b]	5920
T_{eff2} (K)	6004 ± 4
q (m_2 / m_1)	0.341 ± 0.001
A[b]	0.5
g[b]	0.32
$\Omega_1 = \Omega_2$	2.528 ± 0.001
i°	63.07 ± 0.06
$L_1 / (L_1 + L_2)_B$[c]	0.7016 ± 0.0001
$L_1 / (L_1 + L_2)_V$	0.7071 ± 0.0001
$L_1 / (L_1 + L_2)_{R_c}$	0.7095 ± 0.0001
r_1 (pole)	0.4510 ± 0.0004
r_1 (side)	0.4846 ± 0.0005
r_1 (back)	0.5124 ± 0.0006
r_2 (pole)	0.2764 ± 0.0011
r_2 (side)	0.2888 ± 0.0014
r_2 (back)	0.3259 ± 0.0025
Fill-out factor	13.1%
RMS (B)[d]	0.00982
RMS (V)[d]	0.00699
RMS (R_c)[d]	0.00636

a. All error estimates from WDWINTV5.6A (Nelson 2009).
b. Fixed during DC.
c. L_1 and L_2 refer to luminosities of the primary (cooler) and secondary stars, respectively.
d. Monochromatic root mean square deviation of model fit from observed values (mag).

Table 6. Mean absolute parameters (±SD) for GM CVn using mass ratio ($q = m_2/m_1$) and total mass results from the simultaneous Roche model fits of LC and RV data.

Parameter	*Primary*	*Secondary*
Mass ($M_\odot$)	1.23 ± 0.06	0.42 ± 0.02
Radius ($R_\odot$)	1.21 ± 0.02	0.74 ± 0.01
a ($R_\odot$)	2.55 ± 0.04	—
Luminosity ($L_\odot$)	1.62 ± 0.06	0.64 ± 0.02
M_{bol}	4.23 ± 0.04	5.23 ± 0.04
Log (g)	4.36 ± 0.03	4.32 ± 0.03

3.8. Distance estimates to GM CVn

The bolometric magnitudes ($M_{bol1,2}$) and luminosity in solar units ($L_{\odot}$) for the primary (L_1) and secondary stars (L_2) were calculated from well-known relationships where:

$$M_{bol1,2} = 4.75 - 5 \log (R_{1,2} / R_{\odot}) - 10 \log (T_{1,2} / T_{\odot}), \quad (7)$$

and

$$L_{1,2} = (R_{1,2} / R_{\odot})^2 (T_{1,2} / T_{\odot})^4. \quad (8)$$

Assuming that $T_{eff1} = 5920$ K, $T_{eff2} = 6004$ K, and $T_{\odot} = 5772$ K, the solar luminosities for the primary and secondary are $L_1 = 1.62 \pm 0.06$ and $L_2 = 0.64 \pm 0.02$, respectively. Bolometric magnitudes were calculated to be $M_{bol1} = 4.23 \pm 0.04$ and $M_{bol2} = 5.23 \pm 0.04$. Combining the bolometric magnitudes resulted in an absolute value ($M_V = 3.95 \pm 0.04$) when adjusted with the bolometric correction (BC = –0.090) interpolated from Pecaut and Mamajek (2013). Substituting into the Equation 9, the distance modulus:

$$d(pc) = 10^{(m - M_V - A_V + 5) / 5)}, \quad (9)$$

where m = V_{max} (10.18 ± 0.01) and $A_V = 0.024$, leads to an estimated distance of 174 ± 3 pc to GM CVn. This value is about 10% lower than the distance (191 ± 9 pc) calculated directly from the first release (DR-1) of parallax data from the Gaia mission (Lindegren *et al.* 2016). The distance to GM CVn was also estimated using two different empirical relationships derived from calibrated models for contact binaries. Mateo and Ruciński (2017) recently developed a relationship between orbital period (0.275 < P < 0.575 d) and distance (Tycho-Gaia Astronomic Solution parallax data) from a subset of contact binaries which showed that the absolute magnitude (M_V) can be estimated with the expression:

$$M_V = (-8.67 \pm 0.65) (\log(P) + 0.4) + (3.73 \pm 0.06). \quad (10)$$

Using this relationship the absolute magnitude was calculated to be $M_V = 4.04 \pm 0.06$, which upon substitution into Equation 9 yielded a distance of 168 ± 5 pc. A third value for distance (169 ± 33 pc) was derived from a ROTSE-1 catalog of contact binary stars (Gettel *et al.* 2006) in accordance with the empirically derived expression:

$$\log (d) = 0.2V_{max} - 0.18 \log(P) - 1.6 (J\text{–}H) + 0.56, \quad (11)$$

where d is distance in parsecs, P is the orbital period in days, and (J–H) is the 2MASS color for GM CVn. Collectively, the mean distance to this system is therefore estimated to be 175 ± 9 pc.

4. Conclusions

Three new times of minimum were observed based on CCD data collected through B, V, and R_c filters; these along with other published values led to an updated linear ephemeris for GM CVn. Potential changes in orbital periodicity were assessed using eclipse timings which unfortunately only cover a 12-year time period. A straight line relationship between the observed and predicted times of minimum suggests that since 2005 no significant change in the orbital period has occurred. The intrinsic color, $(B\text{–}V)_0$, determined from this study and eight surveys indicates that the effective temperature for the primary is ~5920 K, which corresponds to spectral class F9V-G0V. Radial velocity findings are reported for the first time herein and resulted in a robust solution for the mass ratio (q = 0.341 ± 0.001) after simultaneously modeling with the 2013 LC data. Furthermore, these Roche model simulations revealed that GM CVn is a shallow contact W-type W UMa variable. This system is a worthy candidate for further study to advance our knowledge about the evolutionary track of shallow contact binary systems.

5. Acknowledgements

This research has made use of the SIMBAD database operated at Centre de Données astronomiques de Strasbourg, France. Time-of-minima data from the IBVS website proved invaluable to the assessment of potential period changes experienced by this variable star. In addition, the Northern Sky Variability Survey hosted by the Los Alamos National Laboratory and the International Variable Star Index maintained by the AAVSO (Watson *et al.* 2014) were mined for valuable information. The diligence and dedication shown by all associated with these organizations is very much appreciated. R.H.N. wishes to thank the staff members at the DAO (Dmitry Monin, David Bohlender, and the late Les Saddlmyer) for their usual splendid help and assistance. We very much appreciate the critical review and useful commentary provided by the referee assigned to this paper.

References

Akerlof, C., *et al.* 2000, *Astron. J.*, **119**, 1901.

Amôres, E. B., and Lépine, J. R. D. 2005, *Astron. J.*, **130**, 659.

Applegate, J. H. 1992, *Astrophys. J.*, **385**, 621.

Bahar, E., *et al.* 2017, *Inf. Bull. Var. Stars*, No. 6209, 1.

Berry, R., and Burnell, J. 2005, "Astronomical Image Processing for Windows," version 2.4.0, provided with *The Handbook of Astronomical Image Processing*, 2nd ed., Willmann-Bell, Richmond, VA.

Blättler, E., and Diethelm, R. 2006, *Inf. Bull. Var. Stars*, No. 5699, 1.

Bradstreet, D. H. 2005, in *The Society for Astronomical Sciences 24th Annual Symposium on Telescope Science*, The Society for Astronomical Sciences, Rancho Cucamonga, CA, 23.

Bradstreet, D. H., and Guinan, E. F. 1994, in *Interacting Binary Stars*, ed. A. W. Shafter, ASP Conf. Ser. 56, Astronomical Society of the Pacific, San Francisco, 228.

Bradstreet, D. H., and Steelman, D. P. 2002, *Bull. Amer. Astron. Soc.*, 34, 1224.

Csizmadia, Sz., and Klagyivik, P. 2004, *Astron. Astrophys.*, **426**, 1001.

Diethelm, R. 2006, *Inf. Bull. Var. Stars*, No. 5713, 1.

Diethelm, R. 2007, *Inf. Bull. Var. Stars*, No. 5781, 1.

Diethelm, R. 2010, *Inf. Bull. Var. Stars*, No. 5920, 1.

Eggleton, P. P. 1983, *Astrophys. J.*, **268**, 368.
Gettel, S. J., Geske, M. T., and McKay, T. A. 2006, *Astron. J.*, **131**, 621.
Harris, A. W., *et al.* 1989, *Icarus*, **77**, 171.
He, J.-J., and Qian, S.-B. 2009, in *The Eighth Pacific Rim Conference on Stellar Astrophysics: A Tribute to Kam-Ching Leung*, eds. B. Soonthornthum, S. Komonjinda, K.S. Cheng, K.C. Leung, ASP Conf. Ser. 404, Astronomical Society of the Pacific, San Francisco, 194.
Hübscher, J. 2013, *Inf. Bull. Var. Stars*, No. 6084, 1.
Hübscher, J. 2017, *Inf. Bull. Var. Stars*, No. 6196, 1.
Hübscher, J., and Lehmann, P. B. 2013, *Inf. Bull. Var. Stars*, No. 6070, 1.
Kallrath, J., and Milone, E. F. 1999, *Eclipsing Binary Stars: Modeling and Analysis*, Springer, New York.
Kurucz, R. L. 2000, Baltic Astron., 11, 101.
Kwee, K. K., and van Woerden, H. 1956, *Bull. Astron. Inst. Netherlands*, **12**, 327.
Lindegren, L., *et al.* 2016, *Astron. Astrophys.*, **595A**, 4.
Liu, L., Qian, S.-B., He, J.-J., Li, L.-J., and Liao, W.-P. 2010, *Publ. Astron Soc. Japan*, **62**, 81.
Liu, L., Qian, S.-B., He, J.-J., Li, L.-J., Zhao, E.-G., Jiang, L.-Q., and Han, Z.-T. 2016, *New Astron.*, **43**, 1.
Lucy, L. B. 1967, *Z. Astrophys.*, 65, 89.
Mateo, N. M., and Ruciński, S. M. 2017, *Astron. J.*, **154**, 125.
Minor Planet Observer. 2015, MPO Software Suite (http://www.minorplanetobserver.com), BDW Publishing, Colorado Springs.
Nelson, R. H. 2009, WDWINT56A: Astronomy Software by Bob Nelson (https://www.variablestarssouth.org/bob-nelson).
Nelson, R. H. 2010a, in *The Alt-Az Initiative, Telescope Mirror & Instrument Developments*, eds. R. M. Genet, J. M. Johnson, V. Wallen, Collins Foundation Press, Santa Margarita, CA.
Nelson, R. H. 2010b, *Inf. Bull. Var. Stars*, No. 5929, 1.
Nelson, R. H. 2010c, RAVERE: Astronomy Software by Bob Nelson (https://www.variablestarssouth.org/bob-nelson/).
Nelson, R. H. 2011, *Inf. Bull. Var. Stars*, No. 5966, 1.
Nelson, R. H. 2013a, *Inf. Bull. Var. Stars*, No. 6050, 1.
Nelson, R. H. 2013b, BROAD: Astronomy Software by Bob Nelson (https://www.variablestarssouth.org/bob-nelson/).
Nelson, R. H. 2015, *Inf. Bull. Var. Stars*, No. 6131, 1.
Nelson, R. H. 2016, *Inf. Bull. Var. Stars*, No. 6164, 1.
Paunzen, E. and Vanmunster, T. 2016, *Astron. Nachr.*, **337**, 239.
Pecaut, M. J., and Mamajek, E. E. 2013, *Astrophys. J., Suppl. Ser.*, **208**, 1.
Prša, A., and Zwitter, T. 2005, *Astrophys. J.*, **628**, 426.
Ruciński, S. M. 1969, *Acta Astron.*, **19**, 245.
Ruciński, S. M. 2004, in *Stellar Rotation*, Proc. IAU Symp. 215, eds. A. Maeder, P. Eenens, Astronomical Society of the Pacific, San Francisco, 17.
Schlafly, E. F., and Finkbeiner, D. P. 2011, *Astrophys. J.*, **737**, 103.
Schlegel, D. J., Finkbeiner, D. P., and Davis, M. 1998, *Astrophys. J.*, **500**, 525.
Schwarzenberg-Czerny, A. 1996, *Astrophys. J., Lett.*, **460**, L107.
Skelton, P. L., and Smits, D. P. 2009, *S. Afr. J. Sci.*, **105**, 120.
Software Bisque. 2011, CCDSOFT CCD control software (http://www.bisque.com).
Van Hamme, W. 1993, *Astrophys. J.*, **106**, 2096.
Warner, B. 2007, *Minor Planet Bull.*, **34**, 113.
Watson, C., Henden, A. A., and Price, C. A. 2014, AAVSO International Variable Star Index VSX (Watson+, 2006-2014; http://www.aavso.org/vsx).
Wilson, R. E. 1990, *Astrophys. J.*, **356**, 613.
Wilson, R. E., and Devinney, E. J., 1971, *Astrophys. J.*, **166**, 605.
Wozniak, P. R., *et al.* 2004, *Astrophys. J.*, **127**, 2436.
Yakut, K., and Eggleton, P. P. 2005, *Astrophys. J.*, **629**, 1055.